Am J Neurodegener Dis 2012;1(2):168-179
www.AJND.us /ISSN:2165-591X/AJND1207002

Original Article

Spatial regulation of interleukin-6 signaling in response to neurodegenerative stressors in the retina

Stephanie M Sims[1], Lauren Holmgren[1], Heather M Cathcart[1], Rebecca M Sappington[1,2]

[1]Department of Ophthalmology and Visual Sciences, [2]Department of Pharmacology, Vanderbilt University School of Medicine, Nashville, TN, USA.

Received July 13, 2012; accepted July 31, 2012; Epub August 1, 2012; published August 15, 2012

Abstract: Neuroinflammation, defined as the induction of immune-related processes within the central nervous system, is recognized as a component of many neurodegenerative disorders, including glaucomatous degeneration of retinal ganglion cells (RGCs). Previous work *in vitro* identified IL-6 as a potential neuroprotective factor for RGCs, particularly those challenged by glaucoma-related stressors. Here we examined the temporal and spatial characteristics of IL-6 signaling in response to two stressors related to RGC neurodegeneration: age and elevated intraocular pressure (IOP). Using ELISA, immunoblotting, immunolabeling and quantitative microscopy, we measured and compared whole retina and RGC-related expression of IL-6 and IL-6Rα in normal retina (young C57), retina susceptible to glaucomatous neurodegeneration (young DBA/2), aging retina (aged C57) and aging retina challenged by elevated IOP (aged DBA/2). We found that: 1) neurodegenerative stressors induce alterations in whole retina expression of IL-6 and IL-6Rα, 2) these whole retina changes do not reflect the immediate milieu of RGCs, where IL-6 and IL-6Rα expression is spatially variable and 3) the extent and magnitude of this spatial variability is stressor-dependent. Our data provide the first evidence that neurodegenerative stressors produce microenvironments of IL-6 signaling in retina and that the nature and magnitude of spatial regulation is dependent on the identity of the stressor.

Keywords: Retina, DBA/2, interleukin-6, interleukin-6 receptor, glaucoma

Introduction

Neuroinflammation, defined as the induction of immune-related processes within the central nervous system (CNS), is associated with a variety of cellular events, including reactivity of glial cells (gliosis), infiltration of peripheral immune cells and production of inflammatory cytokines. These events are recognized as a component of many neurodegenerative disorders and are thought to be contributors to age-related decline in neuronal function and survival [1-7]. In retina, neuroinflammation is associated with variety of retinal neurodegenerations, including glaucomatous degeneration of retinal ganglion cells (RGCs).[4,8-16]. Although expression of neuroinflammatory cytokines generally exacerbates retinal neurodegeneration [4,17-22], the inflammatory cytokine interleukin-6 (IL-6) has emerged as a potential neuroprotective factor for retinal ganglion cells (RGCs) *in vitro* and is expressed constitutively in the retina [23-25]. IL-6 is a pleiotropic cytokine, which shares a common signal transduction component (gp130), with other IL-6 family member ligands [26-28]. Specific IL-6 signaling involves interaction of gp130 with membrane-bound IL-6 receptor alpha (IL-6Rα). The IL-6Rα-gp130 receptor complex forms the complete interleukin-6 receptor, which results in downstream transcriptional regulation of pro- and anti-apoptotic factors [27-29]. Despite evidence that retinal expression of IL-6 is sensitive to a variety of neurodegenerative stressors, little is known about the specific nature of these changes or corresponding changes in its receptor.

Here we examined the spatial and temporal characteristics of retinal IL-6 signaling in response to two neurodegenerative stressors associated with RGC degeneration – age and elevated intraocular pressure (IOP). We measured and compared whole retina and RGC-related expression of IL-6 and IL-6Rα in normal retina (young C57), retina susceptible to glaucomatous neurodegeneration (young DBA/2), aging

retina (aged C57) and aging retina challenged by elevated IOP (aged DBA/2). In DBA/2 mice, elevated IOP is naturally induced by the presence of mutations in two genes: gpnmb and tyrp1 [30, 31]. These mutations induce age-related iris atrophy and dispersion of iris pigment that leads to an obstruction of aqueous outflow canals and subsequent elevation in IOP [32]. This elevation in IOP leads to the degeneration of RGCs and their axons in the optic nerve, like that observed in the human condition of glaucomatous optic neuropathy [11, 33, 34]. Although significant pathology is typically not noted in DBA/2 retina until later in the life span, young DBA/2 mice still possess the genotype that leads to IOP elevation and RGC degeneration. As such, young DBA/2 mice are in a state of genetic susceptibility to retinal neurodegeneration. Our studies revealed that: 1) neurodegenerative stressors induce alterations in whole retina expression of IL-6 and IL-6Rα, 2) these whole retina changes do not reflect the immediate milieu of RGCs, where IL-6 and IL-6Rα expression is spatially variable and 3) the extent and magnitude of this spatial variability is stressor-dependent. Together, these data suggest that IL-6 signaling is: 1) spatially regulated in retina and 2) likely to occur in the context of microenvironments, where the magnitude and therefore, impact of IL-6 signaling differs between populations of RGCs within the same retina.

Materials and methods

Animals and tissue preparation

The experimental procedures described were approved by the Vanderbilt University Medical Center Institutional Animal Care and Use Committee. For whole retina protein analysis (ELISA and immunoblotting), retina from young (3 month, n=13) and aged (8 month, n=10) DBA/2 mice were compared to age-matched C57BL/6 (C57, Charles River Laboratories, Wilmington, MA, n=18). The average IOP for DBA/2 mice was 14mmHg +/- 0.84mmHg and 20mmHg +/- 1.55mmHg for three and eight month aged mice, respectively. For immunohistochemical studies, young (2-3 month, n=9) and aged (10-12 month, n=12) DBA/2 mice were compared to age-matched C57BL/6 mice (Charles River Laboratories, n=7). The average IOP for DBA/2 mice was 13mmHg +/- 1.34mmHg and 23mmHg +/- 5.24mmHg for young and aged mice, respectively. IOP was monitored monthly in DBA/2 mice using a tonometer (Tono-Pen; Reichert, Depew, NY) before mice were sacrificed [9, 33, 35].

Enzyme linked immunosorbent assay (ELISA)

Total protein was isolated from freshly dissected retina of three and eight month aged C57BL/6 and DBA/2 mice by homogenization using ultrasonication (1 retina/50μL) in a solution containing 50 mM Tris HCL, pH 7.2 (Cellgro by Mediatech, Manassas, VA), 150mM NaCl (Cellgro), 1% NP-40, 0.25% sodium deoxycholate (Sigma-Aldrich), 100μm PMSF (Sigma-Aldrich), 0.1% SDS (Promega, Madison, WI) and protease/phosphatase inhibitor cocktail (Roche, Branchburg, NJ). Cellular debris was pelted by centrifugation at 14,000 rpm for 30 minutes at 4°C. Protein concentration was determined from the supernatant using a BCA assay (Thermo Fisher Scientific, Waltham, MA). We used an ELISA kit (Quantikine mouse IL-6; R&D Systems; Minneapolis, MN) to measure the concentration of IL-6 in total protein lysate from each retina. The ELISA was conducted according to manufacturer's recommendations. The concentration of IL-6 in each sample was interpolated by a comparison of the optical densities in the sample wells to those of the IL-6 standard curve (0-500pg/ml of IL-6). The minimum detectable level of mouse IL-6 was 1.3-1.8 pg/ml. IL-6 protein concentrations were normalized to μg of total protein.

Immunoblotting

Immunoblotting against IL-6Rα was performed in freshly dissected retina of three and eight month aged C57BL/6 and DBA/2 mice, as previously described [36]. Briefly, single retinas were homogenized in 50mM Tris, pH 6.8, 2% SDS, 10% glycerol, 100mM DTT, 2mM EDTA, 50mM NaF, 0.2mM Na3VO4, 0.25mM PMSF, and protease inhibitor cocktail (Roche). Protein concentration was determined from the supernatant using a BCA assay (Thermo Fisher Scientific). Samples (60-80μg of protein) were prepared in denaturing buffer containing: 100mM Tris-HCl, pH 6.8, 4% SDS, 20% glycerol, 0.2% bromophenol blue, and 200mM dithiothreitol and separated by SDS-PAGE in 4-20% gradient Tris-glycine pre-cast gel (Bio-Rad) and transferred to a PVDF membrane (Millipore; Temecula, CA). The membrane was incubated for one

hour in blocking solution containing: 5% powdered milk and 0.05% Tween-20, pH 7.6. This was followed by an overnight incubation at 4°C in anti-mouse IL-6R/CD126 (2μg/ml; catalog number MAB18301; R and D Systems) and/or anti-β-actin (3μg/ml; catalog number AM4302; Ambion). Following washes in a solution of phosphate-buffered saline (PBS; Fisher Scientific; Fairlawn, NJ) with 0.05% Tween-20, membranes were incubated for 1 hour in blocking solution containing goat anti-rat IgG (400ng/ml; Molecular Probes) or goat anti-mouse IgG (400ng/ml; Molecular Probes) conjugated to Alexa Fluor 680. Following washes in PBS + Tween-20, immunoreactive bands were detected by an Odyssey infrared imaging system (Li-Cor, Lincoln, NE).

Whole mount retina immunohistochemistry

Immunohistochemistry in whole mount retina was performed as previously described [9, 36]. Briefly, retina were cryoprotected in a graded sucrose series (10–30%) and then freeze-thawed on dry ice to enhance penetration of the primary antibody. Following washing in PBS, autofluorescence was quenched by placing the retinas in a 0.1% sodium borohydride (Fisher) solution for 30 minutes at room temperature. Subsequently, retinas were rinsed with PBS and incubated in a blocking solution of 5% normal horse serum (NHS; Sigma-Aldrich; St. Louis, MO) and 0.1% Triton X-100 (Fisher) in PBS overnight at 4°C. Following the blocking step, retinas were transferred into a primary antibody solution with 3% NHS and 0.1% Triton X-100 in PBS for 4 days at 4°C. After rinsing in PBS, the retinas were incubated overnight at room temperature with a secondary antibody solution containing 1% NHS and 0.1% Triton X-100. Retinas were rinsed, mounted on glass slides with Fluoromount-G (Fisher) and cover-slipped. The antibodies used for whole mount retina immunolabeling were rabbit anti-IL-6 IgG (188μg/ml; catalog number ab6672, Abcam; Cambridge, MA), rabbit anti-IL-6Rα IgG (4μg/ml; catalog number sc-660; Santa Cruz; Santa Cruz, CA), mouse anti-SMI-31 (1:1000; catalog number SMI-31R; Covance; Princeton, NJ) goat anti-Iba-1 (1.25μg/ml; catalog number ab5076; Abcam) and mouse anti-GFAP (1:500; catalog number MAB360 Millipore)and were visualized using donkey anti-rabbit Alexa 555 or Alexa 488 (10μg/ml; Invitrogen; Eugene, OR), donkey anti-goat Alexa 488 (10μg/ml; Invitrogen) or donkey anti-mouse Dylight 649 (7.5μg/ml; JacksonImmuno Research; West Grove, PA).

Fluorescence microscopy

Whole mount retina imaging was performed through the Vanderbilt University Medical Center Cell Imaging Shared Resource Core. Staining was imaged on an upright confocal microscope (LSM510 META; Carl Zeiss Inc., Thornwood, NY) or an inverted confocal microscope (Olympus FV -1000; Center Valley, PA) equipped with laser scanning fluorescence (blue/green, green/red, red/far-red). Three dimensional z-series images of the retina were acquired using a digital camera and image analysis software (LSM5; Zeiss or FV-10 ASW; Olympus). For each retina, 10 pseudorandom images through the ganglion cell and nerve fiber layers were obtained between mid-periphery and mid-central regions at 63x magnification.

Quantification of digital microscopy

For each of the 10 pseudorandom retinal images , the ganglion cell- and nerve fiber- layers were collapsed into two dimensional images. We used these images to examine IL-6 and IL-6Rα intensity. All measurements were performed using imaging analysis (Image Pro Plus 5.1; Media Cybernetics, Inc; Bethesda, MD). IL-6 and IL-6Rα intensity was calculated as the mean pixel intensity across each image. As such, one value for IL-6 or IL-6Rα intensity was obtained from each of 10 micrographs per retina. IL-6 and IL-6Rα intensity data are presented in arbitrary units of intensity.

Statistical analysis

All statistical tests were performed with SigmaPlot (Systat Software Inc., San Jose, CA). For ELISA and immunoblotting data, mean IL-6 concentrations (pg/ml/μg of total protein) and IL-6Rα/actin ratios were compared among groups using one-way analysis of variance and pairwise multiple comparisons were made between groups using the Holm-Sidak method. For analysis of whole mount expression data, we compared labeling intensity among groups using Kruskal-Wallace one-way analysis of variance followed by post hoc pair-wise comparisons between groups using Dunn's Method. Error bars represent ± SD of the mean. For all analyses, $p \leq 0.05$ was considered statistically significant.

Results

Aging and neurodegenerative stressors impact IL-6 signaling in whole retina

To assess global changes in IL-6 signaling, we quantified IL-6 and IL-6Rα expression in protein lysates from whole retina of DBA/2 and C57 mice, as a function of age. IL-6 levels were the highest in aged C57 mice (0.198pg/ml/μg). This concentration of IL-6 was 1.5 fold higher than in young C57 mice (P=0.007) and 60% higher than DBA/2 mice of the same age ($p < 0.001$; **Figure 1A**). Although there was a trend towards decreasing IL-6 in aged DBA/2 mice compared to young DBA/2 mice, this trend did not reach statistical significance ($p = 0.15$; **Figure 1A**). These data suggest that expression of IL-6 in whole retina increases with normal aging in C57 mice and with a state of susceptibility to neurodegeneration (young DBA/2). However, an age-related increase in IL-6 expression was not observed in DBA/2 mice, suggesting that development of elevated IOP may alter temporal trends in retinal IL-6 expression.

In contrast to IL-6, IL-6Rα levels were highest in young DBA/2 mice (0.0087pg/ml/μg protein) and lowest in young C57 mice (0.0018pg/ml/μg protein; **Figure 1B**). This almost 5-fold difference in IL-6Rα expression level was statistically significant ($p < 0.05$; **Figure 1B**). Similarly, IL-6Rα expression in aged DBA/2 mice was almost 4-fold higher than that of young C57 mice ($p < 0.05$; **Figure 1B**). Interestingly, IL-6Rα expression did not differ in aged C57 and aged DBA/2 mice, compared to their younger counterparts ($p > 0.05$; **Figure 1B**). For IL-6Rα, there was no evidence of an age-related change in expression for either C57 or DBA/2 mice, suggesting that normal aging and the development of a neurodegenerative stressor do not significantly alter IL-6Rα expression levels in whole retina. However, DBA/2 mice in both age groups exhibited higher IL-6Rα expression, suggesting that both the presence of and susceptibility to development of elevated IOP coincides with elevated expression of IL-6Rα.

RGCs are a target of IL-6 signaling in response to IOP and aging stressors

Although our whole retina analysis suggests that both IL-6 and IL-6Rα expression may be altered by the predisposition to and the presence of IOP -induced neurodegeneration, this analysis does not provide information about the relevance of these changes to glaucomatous neurodegeneration. Since cytokines tend to act locally within a relatively small spatial area and RGCs are the specific targets of IOP-induced neurodegeneration, we examined localization of IL-6 and IL-6Rα in the ganglion cell and nerve fiber layers of DBA/2 retina. Confocal microscopy confirmed that IL-6 is present in the extracellular space

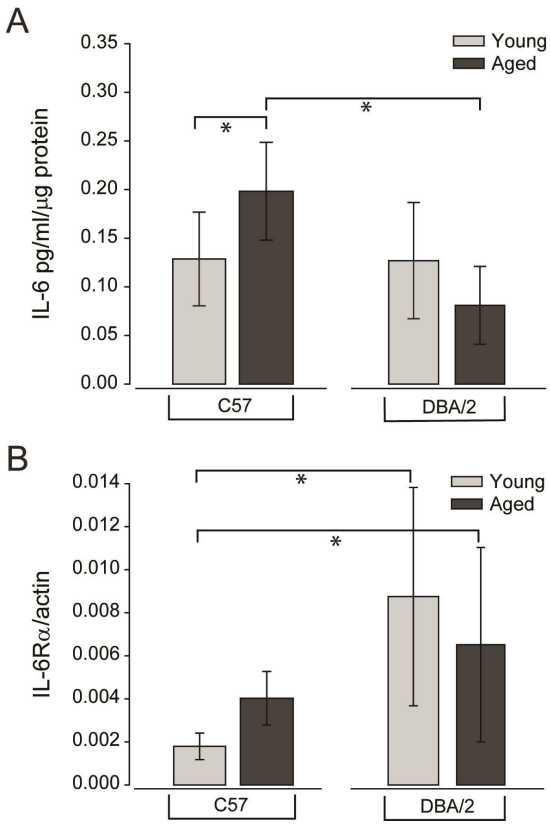

Figure 1. Age- and IOP-related stressors differentially impact IL-6 and IL-6Ra expression in whole retina. Graphical representation of IL-6 (A) and IL-6Rα (B) protein concentration in whole retina lysates from young C57, aged C57, young DBA/2 and aged DBA/2 mice. Asterisks denote $p < 0.05$. A. IL-6 concentration, as measured by ELISA, is depicted as pg/ml/μg of total protein. IL-6 expression in aged C57 mice is 1.5-fold greater than young C57 mice and 60% greater than age-matched DBA/2 mice. IL-6 expression does not increase with age in DBA/2 mice, but rather, trends toward decreasing expression ($p = 0.15$). B. IL-6Rα expression, as measured by immunoblotting is depicted as the ratio of IL-6Rα to actin. IL-6Rα expression was ~5-fold and ~4-fold greater in young DBA/2 retina and aged DBA/2 retina respectively, than in young C57. No significant changes in IL-6Rα expression were noted with aging in either C57 or DBA/2 mice or between aged C57 and DBA/2 retina.

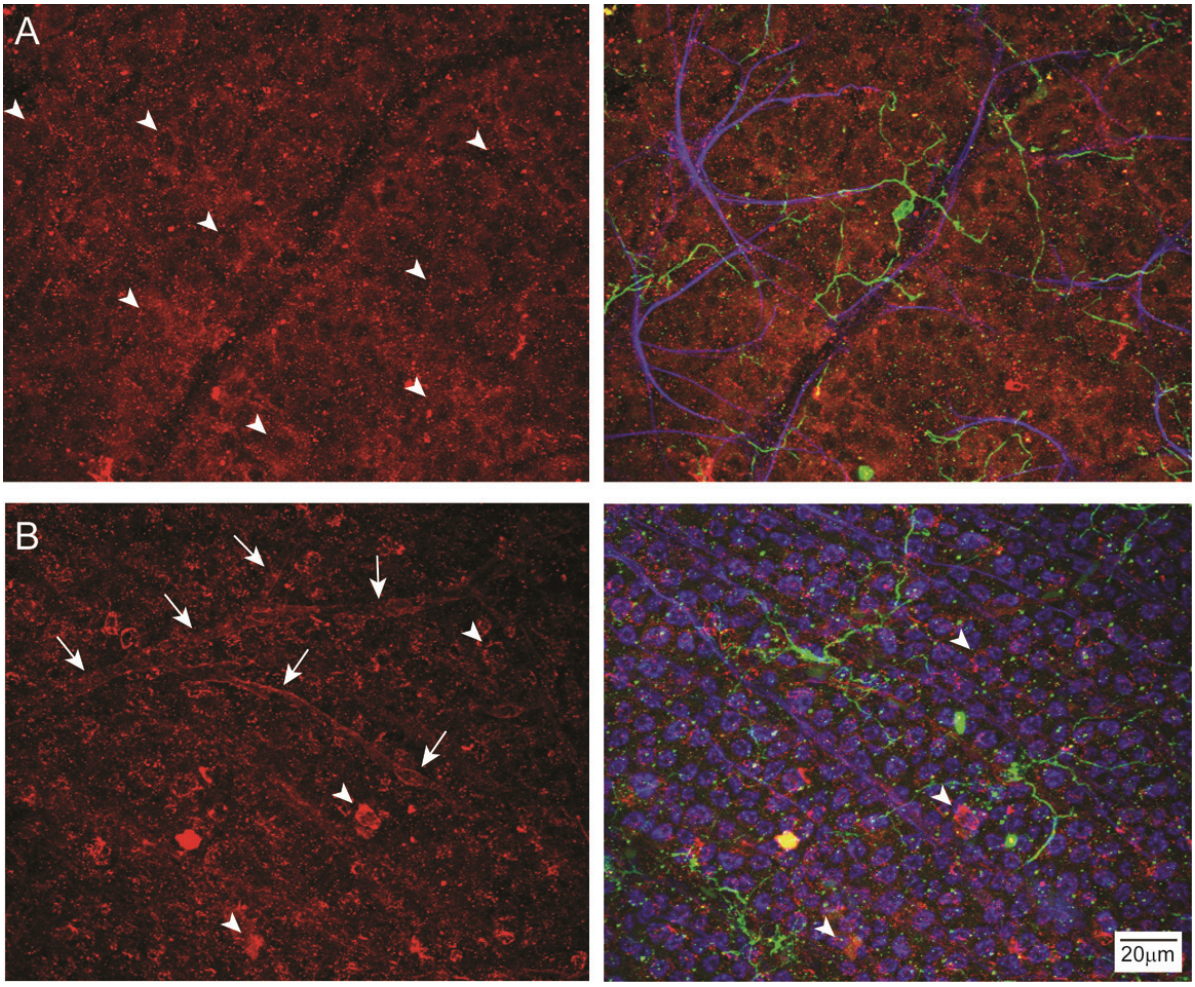

Figure 2. IL-6 localizes primarily to the extracellular space surrounding RGCs, while IL-6Rα localizes primarily to RGCs and retinal vasculature. Confocal micrographs of the ganglion cell and nerve fiber layers of aged DBA/2 retina depicting cell type-specific expression of IL-6 and IL-6Rα. Scale is consistent. **A.** Immunolabeling of IL-6 (left panel; red) reveals primary localization of IL-6 to the extracellular space surrounding RGC soma in the ganglion cell layer (arrowheads). Co-immunolabeling (right panel) of IL-6 (red) with antibodies against the microglia marker Iba-1 (green) and the astrocyte marker GFAP (blue) reveal co-localization of IL-6 and Iba-1 in microglia as well as an association between IL-6 and GFAP+ astrocytes. **B.** Immunolabeling of IL-6Rα (red; left panel) reveals localization to RGC soma (arrowheads) and vasculature (arrows). Co-immunolabeling (right panel) of IL-6Rα (red) with the microglia marker Iba-1 (green) and the RGC marker SMI-31 (blue) reveals co-localization of IL-6Rα with SMI-31 (arrowheads), confirming expression of IL-6Rα by RGCs.

surrounding RGC axons in the nerve fiber layer and RGC soma in the ganglion cell layer of aged DBA/2 mice (**Figure 2A**). Co-immunolabeling with the microglia marker Iba-1 and the astrocyte marker GFAP revealed intracellular localization of IL-6 in Iba-1+ microglia and an association of extracellular IL-6 with GFAP+ astrocytes (**Figure 2A**). In contrast, IL-6Rα is primarily associated with both RGC soma and axons, as determined by co-localization of IL-6Rα signal with the RGC marker SMI-31 (**Figure 2B**). IL-6Rα also localizes to vasculature in the nerve fiber layer, as determined by morphology (**Figure 2B**). This data confirms previous observations *in vitro* that IL-6 is likely produced by microglia and that RGCs are a target of IL-6 signaling in glaucomatous neurodegeneration [8, 9, 24].

Stressor-dependent changes in IL-6 signaling directly relevant to RGCs differs substantially from that in whole retina

To quantify layer-specific changes in IL-6 and IL-6Rα expression, we performed a spatial analysis by measuring total intensity of IL-6 and IL-6Rα immunolabel in the ganglion cell and nerve

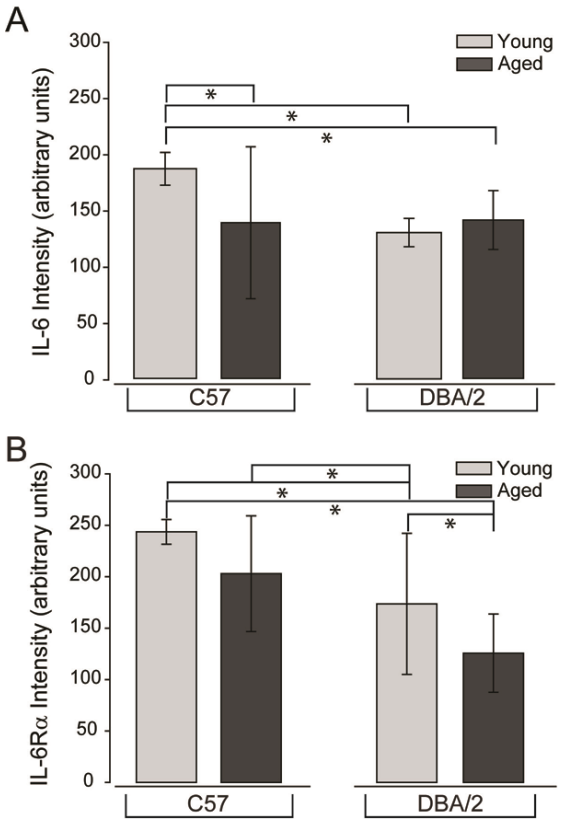

Figure 3. Age and elevated IOP differentially modulate layer-specific expression of both IL-6 and IL-6Rα. Graphical representation of mean intensity of IL-6 (**A**) and IL-6Rα (**B**) labeling in the ganglion cell and nerve fiber layers of age-matched, young and aged C57 and DBA/2 mice. Asterisks denote statistical significance of $p \leq 0.05$. **A.** Young C57 retina exhibited 24-30% more IL-6 labeling than all other conditions, including aged C57 retina. There is no significant difference in the intensity of IL-6 labeling between aged C57, young DBA/2 or aged DBA/2 retina. **B.** IL-6Rα labeling intensity was highest in young C57 retina and lowest in aged DBA/2 retina, with aged DBA/2 retina exhibiting as much as 48% less label than all other conditions. Although there is no significant difference between young and aged C57 retina, aged DBA/2 retina exhibits 28% less IL-6Rα labeling than young DBA/2 retina.

fiber layers of 10 pseudorandom, confocal micrographs per retina. Quantification of mean IL-6 labeling within the ganglion cell and nerve fiber layers revealed that young C57 mice exhibit the highest mean intensity, which was 26% greater than aged C57 ($p < 0.05$), 24% greater than aged DBA/2 and 30% greater than age-matched DBA/2 ($P < 0.05$; **Figure 3A**). There was no significant difference in IL-6 intensity between aged C57, aged DBA/2 and young DBA/2 retinas. These data suggest that the collective expression of IL-6 in the ganglion cell and nerve fiber layers of the retina diminishes with aging in both the presence (aged DBA/2) or absence (aged C57) of a neurodegenerative stressor, as well as, in retina from young mice predisposed to the development of neurodegenerative stressor (young DBA/2).

Similar to IL-6, IL-6Rα expression was greatest in the ganglion cell and nerve fiber layers of C57 mice. However, this expression did not differ significantly with age ($p > 0.05$; **Figure 3B**). IL-6Rα expression in young DBA/2 retina was 29% and 14% less than young and aged C57 retina, respectively ($p < 0.05$). Aged DBA/2 mice exhibited the lowest IL-6Rα expression, which was 48% less than young C57, 38% less than aged C57 and 28% less than young DBA/2 ($p > 0.05$; **Figure 3B**). These data suggest that while aging alone does not significantly impact IL-6Rα expression by RGCs, the combination of aging and elevated IOP serves to reduce this expression. Interestingly, young DBA/2 mice also exhibited reduced IL-6Rα expression by RGCs, suggesting that the capacity for IL-6 signaling is reduced in RGCs prior to presentation of the IOP stressor and onset of neurodegeneration.

IL-6 signaling is spatially regulated into discreet microenvironments that vary by stressor

Our layer-specific analysis of IL-6 and IL-6Rα expression provided an assessment of IL-6 signaling that was more relevant to RGCs than the whole retina analysis. However, we noted that despite the restriction of our analysis to the ganglion cell and nerve fiber layers, significant variability from the mean remained. Examination of IL-6 and IL-6Rα staining patterns across the entire ganglion cell and nerve fiber layers of the retina revealed a mosaic pattern of labeling intensities within each individual retina. This mosaic pattern consisted of areas of high intensity labeling intermixed with areas of lower intensity labeling. Qualitatively, IL-6 labeling was most consistent in young C57 retina (**Figure 4A**) with spatial variability noted in aged C57 (**Figure 4B**), young DBA/2 (**Figure 4C**) and aged DBA/2 retina (**Figure 4D**). Similarly, IL-6Rα labeling was also most consistent in young C57 retina (**Figure 5A**), while aged C57 (**Figure 5B**), young DBA/2 (**Figure 5C**) and aged DBA/2 retina (Figure 5D)

all exhibited significant spatial variability.

To more specifically assess trends in spatial variation of IL-6 and IL-6Rα labeling, we performed histogram and variation analysis of labeling intensities from the individual micrographs used for mean analysis (**Figure 6**) and compared the histogram functions between C57 and DBA/2 mice in both age groups. Histogram analysis revealed that IL-6 labeling was fairly consistent in both young C57 and young DBA/2 retina (**Figure 6A**). However, the histogram function for young C57 retina was shifted to the right reflecting the overall higher intensity of IL-6 labeling in these retina (180-210 intensity units). For young DBA/2 retina, the histogram function was slightly broader and concentrated in more moderate intensities (110-160 intensity units). Similarly, the histogram function for aged DBA/2 retina was also heavily concentrated in the moderate range exhibited by young DBA/2 retina (110-160 intensity units). However, these retina also exhibited a few instances of low intensity (90-100 intensity units) and high intensity (170-200 intensity units) labeling leading to a broader overall distribution (**Figure 6A**). The broadest histogram function was observed in aged C57 retina, where labeling intensities ranged from 60–250 intensity units (Figure 6A). Interestingly, the distribution across these intensities was rather even without the obvious spikes noted in all other groups (Figure 6A). Mathematical assessment of variation in IL-6 intensities revealed that the coefficient of variability was least in young C57 (0.078) and young DBA/2 retina (0.097). The variability in aged DBA/2 retina (0.186) was approximately 2 -fold higher than that of both young C57 and young DBA/2 retina. The greatest variability was noted in aged C57 retina, which exhibited a coefficient of variability of 0.448. This degree of variability was almost 2-fold greater than that of age-matched DBA/2 retina and more than 5-fold higher than that of young C57 and young DBA/2 retina. This data confirms our qualitative and histogram analysis of spatial variability in IL -6 expression illustrating the smallest degree of variability in young C57 and DBA/2 retina and greatest in aged C57 retina with aged DBA/2 mice falling into a more moderate range.

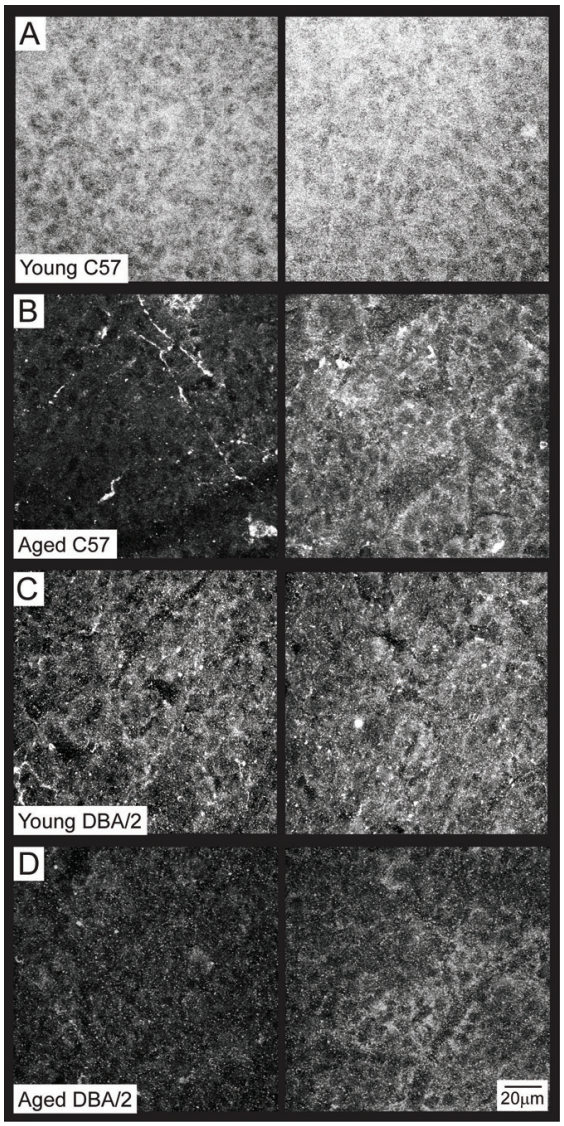

Figure 4. IL-6 in the ganglion cell and nerve fiber layers of the retina exhibits a distinct mosaic pattern of localization, particularly with age. **A-D.** Representative confocal micrographs of IL-6 immunolabeling in the ganglion cell and nerve fiber layers of whole-mount retina from young C57 (**A**), aged C57 (**B**), young DBA/2 (**C**) and aged DBA/2 (**D**) mice. Confocal micrographs are a single projection of micrographs stacked in the z-plane to encompass the entirety of the ganglion cell and nerve fiber layers. IL-6 immunostaining presents in a mosaic pattern of varying labeling intensities across the retina. The left and right panels are representative micrographs of the degree of labeling variation noted within a single retina, where the left panel demonstrates the lowest labeling intensity and the right panel demonstrates the highest labeling intensity for each retina. Qualitative comparisons of the left and right panels within each experimental group reveal that IL-6 labeling is most consistent in young C57 retina (**A**) and most variable in aged C57 retina (**B**), with young (**C**) and aged (**D**) DBA/2 retina exhibiting moderate levels of spatial variability. Scale is consistent for A-D.

Similar to IL-6, the histogram function for IL-6Rα was tightest in young C57 retina and skewed to the right (225-262 intensity units), reflecting higher expression levels of IL-6Rα with little spatial variability (**Figure 6B**). In contrast, the histogram functions for aged C57, young DBA/2 and aged DBA/2 retina were widespread, indicating significant spatial variability for each of these conditions (**Figure 6B**). Of these histogram functions, aged C57 and aged DBA/2 retina exhibited the most even distribution of IL-6Rα labeling intensities, with a slight shift to the left for aged DBA/2 retina (85-225 versus 85-255 intensity units) reflecting the overall lower level of IL-6Rα expression in these mice (**Figure 6B**). Interestingly, young DBA/2 retina exhibited a more bimodal distribution with a majority of fields concentrated in either low intensity (85-125 intensity units) or high intensity regions (237-262; **Figure 6B**). The coefficients of variability for young DBA/2 (0.395), aged C57 (0.277) and aged DBA/2 mice (0.303) were between 5.6-fold and 8-fold greater than young C57 retina (0.049), with young DBA/2 mice exhibiting the greatest extent of variability. This confirmed both our qualitative and histogram data, which suggested that spatial variation in IL-6Rα expression was least in young C57 retina and greatest in young DBA/2 retina with aged C57 and aged DBA/2 mice falling into more moderate ranges.

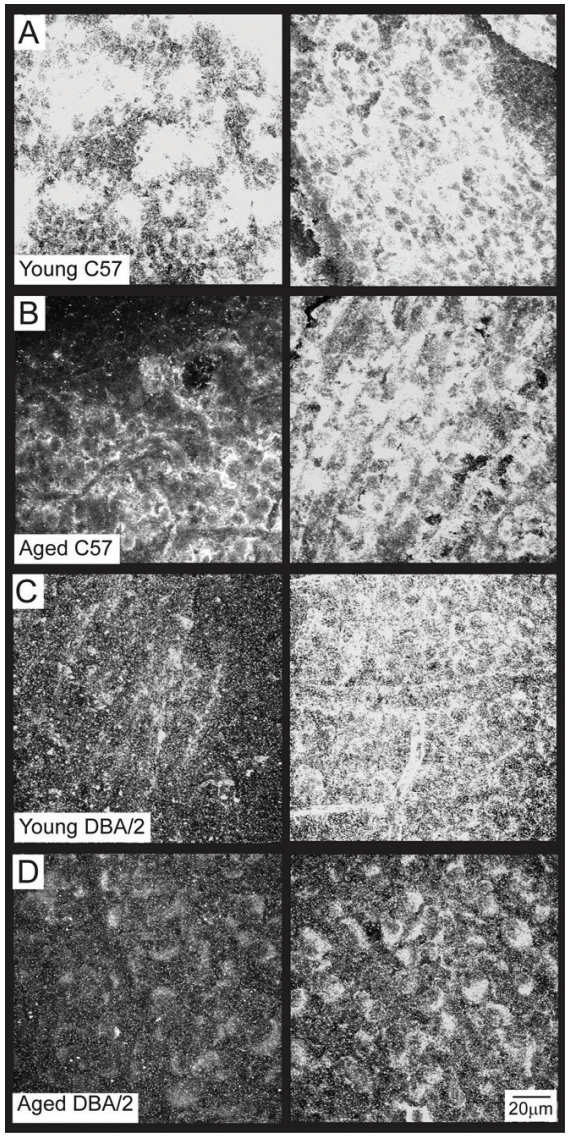

Together, these data support the observation that IL-6 and IL-6Rα expression can vary across discreet spatial areas, not only within individual retinas, but also within restricted regions prone to age-related neurodegeneration. That retinas from young C57 mice exhibit less of these spatial variations than DBA/2 retina and their aged C57 counterparts, suggests that the development of discreet, spatial variations in IL-6 signaling are relevant to both aging- and degeneration-related pathobiology.

Discussion

Neuroinflammation is recognized as a component of many neurodegenerative disorders, including glaucomatous neurodegeneration of

Figure 5. IL-6Rα in the ganglion cell and nerve fiber layers of the retina exhibits a distinct mosaic pattern of localization, particularly with neurodegenerative stressors. **A-D.** Representative confocal micrographs of IL-6Rα immunolabeling in the ganglion cell and nerve fiber layers of whole mount retina from young C57 (**A**), aged C57 (**B**), young DBA/2 (**C**) and aged DBA/2 (**D**) mice. Confocal micrographs are a single projection of micrographs stacked in the z-plane to encompass the entirety of the ganglion cell and nerve fiber layers. IL-6Rα immunostaining presents in a mosaic pattern of varying labeling intensities across the retina. The left and right panels are representative micrographs of the degree of labeling variations noted within a single retina, where the left panel demonstrates the lowest labeling intensity and the right panel demonstrates the highest labeling intensity for each retina. Qualitative comparisons of the left and right panels within each experimental group reveal that IL-6Rα labeling is most consistent in young C57 retina (**A**) and significantly variable in aged C57 (**B**), young DBA/2 retina (**C**) and aged DBA/2 (**D**) retina. Scale is consistent for A-D.

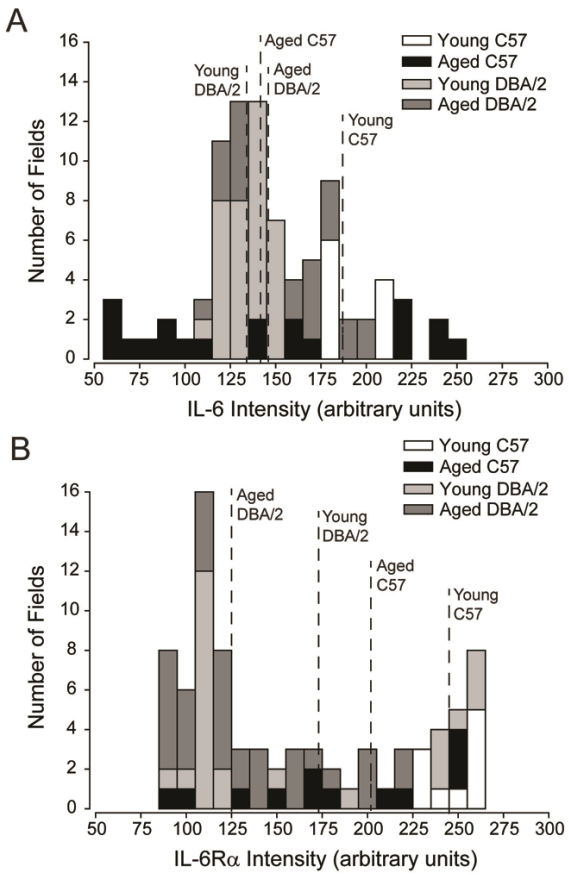

Figure 6. Spatial variability is a significant characteristic of IL-6 signaling that is dependent upon both age and neurodegenerative stressors. Histogram analyses of spatial variability in IL-6 (**A**) and IL-6Rα (**B**) labeling within the ganglion cell and nerve fiber layers of young and aged C57 and DBA/2 retina. Histograms are presented as the number of confocal microscope fields as a function of IL-6 (**A**) or IL-6Rα (**B**) labeling intensity. Dotted lines denote the mean intensity for each group. **A.** As indicated by the breadth of intensities represented in each experimental group, spatial variability is greatest in aged C57 retina and least in young C57 retina. These two groups also represent the lowest and highest extremes in labeling intensities. Young and aged DBA/2 retina both exhibit greater spread of the histogram function than young C57 retina, but less than aged C57 retina, indicating a moderate level of spatial variability for both of these experimental groups. **B.** Young C57 retina exhibits the smallest spread of the histogram, which is concentrated to the right, indicating higher labeling intensities. Aged C57, young DBA/2 and aged DBA/2 retina all exhibit broad histogram functions, but with varying characteristics. While aged C57 retina exhibits a rather uniform range in the incidence of labeling intensities, histogram functions are shifted to the left in aged DBA/2 retina and are more bimodal in young DBA/2 retina with regard to IL-6Rα intensity.

RGCs [2-5,8-16]. Previous work *in vitro* identified IL-6 as a potential neuroprotective factor for RGCs [23-25]. Here we examined IL-6 signaling in response to two neurodegenerative stressors associated with RGC degeneration: aging and elevated IOP [11, 34]. For our studies, we examined the temporal and spatial characteristics of IL-6 signaling in normal retina (young C57), retina susceptible to neurodegeneration (young DBA/2), aging retina (aged C57) and aging retina challenged by an IOP stressor (aged DBA/2). By comparing expression and localization patterns of IL-6 and IL-6Rα, we identified characteristics of IL-6 signaling unique to each of these conditions.

For constitutive IL-6 signaling in young C57 retina, we noted consistent levels of IL-6 and IL-6Rα expression in whole retina and layer-specific analyses (**Figure**s **1** and **3**). Although there was some variability in the spatial localization of both IL-6 and IL-6Rα in young C57, this level of variability was far less than that observed in retina challenged by neurodegenerative stressors (**Figure**s **4**-**6**). Overall, these data suggest that constitutive IL-6 signaling occurs in the retina and that its functions are relevant to the entire population of RGCs.

Genetic susceptibility to retinal neurodegeneration (young DBA/2) resulted in a pattern of IL-6 signaling distinctive from constitutive IL-6 signaling in age-matched C57 retina. Whole retina analysis revealed decreased IL-6 expression in young DBA/2 mice that was accompanied by increased IL-6Rα expression (**Figure 1**). This data suggests that despite lower levels of IL-6 expression, young DBA/2 retina actually exhibits a greater sensitivity to IL-6 signaling than age-matched C57 retina. Interestingly, layer-specific analysis revealed that, compared to young C57 retina, both IL-6 and IL-6Rα expression decreased in the immediate milieu of RGCs in young DBA/2 retina (**Figure 3**). This suggests that RGCs do not account for elevations in IL-6Rα expression noted in our whole retina analysis and that IL-6 signaling in RGCs is actually reduced in young DBA/2 retina (**Figure 1**). In terms of localization patterns, spatial variability in IL-6 expression was low and very similar to that of young C57 mice (**Figure**s **4** and **6**). In contrast, spatial variations in IL-6Rα expression were significant with the range of expression levels exceeding the other groups by 2-fold or more (**Figures 5** and **6**). This suggests that genetic susceptibility to retinal neurodegeneration

is sufficient to induce spatial regulation of IL-6 signaling. Interestingly, this spatial regulation occurs not through the spatial availability of IL-6, but more so, by expression of its receptor on the target cell. Whether alterations in the extent and regulation of IL-6 signaling results from IOP-related mutations or from other aspects of the strain genome, is difficult to ascertain. In either case, their existence opens the possibility that neuroinflammatory processes, like IL-6 signaling, may be indicators of future pathology that could serve to "prime" the system for neurodegeneration. This notion has been proposed by others elsewhere in the CNS [1, 7, 37-40].

Aging stressors alone, as evaluated in C57 retina, also resulted in a pattern of IL-6 signaling distinctive from constitutive IL-6 signaling in young retina. In aged C57 retina compared to young C57 retina, whole retina expression of IL-6 increased, while IL-6Rα expression remained unaltered (**Figure 1**). This suggests that while global levels of IL-6 are elevated in aging retina, the capacity of the retina to respond to IL-6 signaling remains unchanged. Contrary to whole retina analysis, layer-specific analysis revealed that IL-6 expression near RGCs actually decreased with age in C57 mice. This suggests that RGCs are not the primary targets of whole retina elevations in IL-6 expression (**Figure 3**). However, in agreement with our whole retina analysis, layer-specific expression of IL-6Rα remained unaltered with age, indicating that receptivity of RGCs to IL-6 remains unaltered (**Figure 3**). Aging stressors in C57 retina also induced significant spatial variability in the localization of IL-6 and IL-6Rα within the ganglion cell and nerve fiber layers. Interestingly, normal aging actually induced the greatest variability in IL-6 expression compared to all other conditions (Figures 4 and 6). This level of high variability in IL-6 expression was coincident with a more moderate level of variability in IL-6Rα expression (62% < IL-6 variability). These data suggest that: 1) stressors associated with normal aging result in spatial regulation of IL-6 signaling and 2) this spatial regulation is attributable more to the expression pattern of the IL-6 ligand than to expression of the receptor by the target cells.

The combination of aging and IOP stressors in aged DBA/2 retina induced changes in IL-6 signaling that shared characteristics with both normal aging (aged C57) and a state of susceptibility to neurodegeneration (young DBA/2). In aged DBA/2 retina, both the global and layer-specific expression of IL-6 was reduced to levels comparable to both aged C57 and young DBA/2 retina (**Figures 1** and **3**). Similar to young DBA/2 retina, global IL-6Rα levels were elevated, but layer-specific IL-6Rα levels were reduced. This suggests that both the presence of and a predisposition to a neurodegenerative stressor decreases the capacity of RGCs specifically to respond to IL-6 signaling (**Figures 1** and **3**). Interestingly, IL-6Rα levels in the immediate milieu of RGCs were lowest in aged DBA/2 retina compared to all other conditions, suggesting that responsiveness to IL-6 is directly related to the magnitude of the stressor. Like aged C57 and young DBA/2 retina, aged DBA/2 retina also exhibited spatial variability in the localization patterns of IL-6 and IL-6Rα. Compared to other conditions, aged DBA/2 retina exhibited moderate levels of variability in spatial patterns of IL-6 and IL-6Rα expression. However, the extent of variability was 62% greater in IL-6Rα expression than in IL-6 expression, a disparity almost identical to the reverse relationship noted in aged C57 retina. This suggests that the presence of a neurodegenerative stressor shifts the mechanisms that govern spatial regulation of IL-6 signaling from ligand-based in normal aging to receptor-based. It is particularly interesting that spatial regulation of IL-6 signaling also appears to be receptor-based in the young DBA/2, which is predisposed to, but not actively experiencing, the IOP stressor.

One caveat to our study lies in the targets of IL-6 signaling in the ganglion cell and nerve fiber layers of the retina. In these layers, IL-6Rα localized to RGC soma and axons and also to vasculature (**Figure 2**). While expression of IL-6Rα was not restricted to RGCs, expression by blood vessels in the nerve fiber layer represented only a small fraction of total IL-6Rα expression in the ganglion cell and nerve fiber layers. Although this does not indicate that IL-6 signaling in blood vessels is inconsequential to the pathobiology of aging and neurodegeneration, it is likely that the changes in IL-6 signaling noted within these layers predominantly reflects IL-6 signaling that targets RGCs. However, it may be advisable to assess vasculature-associated IL-6 signaling with a more targeted experimental approach at a later date.

Overall, these data provide the first evidence that: 1) neurodegenerative stressors produce microenvironments of IL-6 signaling in retina and 2) the nature of this spatial regulation is

dependent on the identity of the stressor. That retina from young C57 mice exhibited less of these spatial variations than DBA/2 retina and their aged C57 counterparts, suggests that the development of these IL-6 microenvironments is a key feature of IL-6 signaling induced by neurodegenerative stressors. The observation of spatial variability in retinal neurodegeneration is not without precedent, particularly in glaucoma, where deficits in RGC axon transport, accumulation of phosphorylated neurofilament and actual loss of RGCs occurs in a sectorial fashion [35, 41-45]. However, it is important to note that the microenvironments of IL-6 signaling described here are more discreet than those observed in RGC survival/function, suggesting that a more refined mechanism underlies this spatial regulation. It is likely that the need for spatial regulation stems from the pleiotropic nature of IL-6 and most other inflammatory cytokines, where tight regulation of their availability is required to target specific cells and control a multitude of downstream effects. However, it is unclear how the location and nature of these microenvironments is determined, as a variety of anatomical, biophysical and biochemical factors could mediate their formation. Furthermore, it is unclear whether formation of these microenvironments constitutes hyper-regulation or dysregulation of IL-6 signaling.

Acknowledgements

These studies were supported by National Institutes of Health Grant R01EY020496 (RMS), NEI Core Grant P30EY08126 (Vanderbilt Vision Research Center) and Research to Prevent Blindness-Career Development Award (RMS).The authors would like to thank David Calkins, PhD and the Vanderbilt University Medical Center Cell Imaging Shared Resource for technical assistance.

Commercial relationships: None

Please address correspondence to: Rebecca M Sappington, PhD, Department of Ophthalmology and Visual Sciences, The Vanderbilt Eye Institute, Vanderbilt University Medical Center, 11445E Medical Research Building IV, Nashville, TN 37232-0654, USA. Tel: 615-322-0790; Fax: 615-936-1594; E-mail: rebecca.m.sappington@vanderbilt.edu

References

[1] Damani MR, Zhao L, Fontainhas AM, Amaral J, Fariss RN and Wong WT. Age-related alterations in the dynamic behavior of microglia. Aging Cell 2011; 10: 263-276.

[2] Morales I, Farias G and Maccioni RB. Neuroimmunomodulation in the pathogenesis of Alzheimer's disease. Neuroimmunomodulation 2010; 17: 202-204.

[3] Brown GC and Neher JJ. Inflammatory neurodegeneration and mechanisms of microglial killing of neurons. Mol Neurobiol 2010; 41: 242-247.

[4] Zhao B and Schwartz JP. Involvement of cytokines in normal CNS development and neurological diseases: recent progress and perspectives. J Neurosci Res 1998; 52: 7-16.

[5] Tansey MG and Goldberg MS. Neuroinflammation in Parkinson's disease: its role in neuronal death and implications for therapeutic intervention. Neurobiol Dis 2010; 37: 510-518.

[6] Campbell IL. Structural and functional impact of the transgenic expression of cytokines in the CNS. Ann N Y Acad Sci 1998; 840: 83-96.

[7] Lynch AM, Murphy KJ, Deighan BF, O'Reilly JA, Gun'ko YK, Cowley TR, Gonzalez-Reyes RE and Lynch MA. The impact of glial activation in the aging brain. Aging Dis 2010; 1: 262-278.

[8] Sappington RM and Calkins DJ. Pressure-induced regulation of IL-6 in retinal glial cells: involvement of the ubiquitin/proteasome pathway and NFkappaB. Invest Ophthalmol Vis Sci 2006; 47: 3860-3869.

[9] Sappington RM and Calkins DJ. Contribution of TRPV1 to microglia-derived IL-6 and NFkappaB translocation with elevated hydrostatic pressure. Invest Ophthalmol Vis Sci 2008; 49: 3004-3017.

[10] Inman DM and Horner PJ. Reactive nonproliferative gliosis predominates in a chronic mouse model of glaucoma. Glia 2007; 55: 942-953.

[11] Coleman AL and Miglior S. Risk factors for glaucoma onset and progression. Surv Ophthalmol 2008; 53 Suppl1: S3-10.

[12] Xu H, Chen M, Mayer EJ, Forrester JV and Dick AD. Turnover of resident retinal microglia in the normal adult mouse. Glia 2007; 55: 1189-1198.

[13] Bosco A, Steele MR and Vetter ML. Early microglia activation in a mouse model of chronic glaucoma. J Comp Neurol 2011; 519: 599-620.

[14] Liou GI. Diabetic retinopathy: Role of inflammation and potential therapies for anti-inflammation. World J Diabetes 2010; 1: 12-18.

[15] Buschini E, Piras A, Nuzzi R and Vercelli A. Age related macular degeneration and drusen: neuroinflammation in the retina. Prog Neurobiol 2011; 95: 14-25.

[16] Yang Z, Quigley HA, Pease ME, Yang Y, Qian J, Valenta D and Zack DJ. Changes in gene expression in experimental glaucoma and optic nerve transection: the equilibrium between protective and detrimental mechanisms. Invest Ophthalmol Vis Sci 2007; 48: 5539-5548.

[17] Tezel G and Wax MB. The immune system and

glaucoma. Curr Opin Ophthalmol 2004; 15: 80-84.
[18] Hernandez MR, Miao H and Lukas T. Astrocytes in glaucomatous optic neuropathy. Prog Brain Res 2008; 173: 353-373.
[19] Tezel G. TNF-alpha signaling in glaucomatous neurodegeneration. Prog Brain Res 2008; 173: 409-421.
[20] Yuan L and Neufeld AH. Tumor necrosis factor-alpha: a potentially neurodestructive cytokine produced by glia in the human glaucomatous optic nerve head. Glia 2000; 32: 42-50.
[21] Tezel G, Li LY, Patil RV and Wax MB. TNF-alpha and TNF-alpha receptor-1 in the retina of normal and glaucomatous eyes. Invest Ophthalmol Vis Sci 2001; 42: 1787-1794.
[22] Langmann T. Microglia activation in retinal degeneration. J Leukoc Biol 2007; 81: 1345-1351.
[23] Mendonca Torres PM and de Araujo EG. Interleukin-6 increases the survival of retinal ganglion cells in vitro. J Neuroimmunol 2001; 117: 43-50.
[24] Sappington RM, Chan M and Calkins DJ. Interleukin-6 protects retinal ganglion cells from pressure-induced death. Invest Ophthalmol Vis Sci 2006; 47: 2932-2942.
[25] Inomata Y, Hirata A, Yonemura N, Koga T, Kido N and Tanihara H. Neuroprotective effects of interleukin-6 on NMDA-induced rat retinal damage. Biochem Biophys Res Commun 2003; 302: 226-232.
[26] Knupfer H and Preiss R. sIL-6R: more than an agonist? Immunol Cell Biol 2008; 86: 87-91.
[27] Taga T and Kishimoto T. Gp130 and the interleukin-6 family of cytokines. Annu Rev Immunol 1997; 15: 797-819.
[28] Rose-John S, Scheller J, Elson G and Jones SA. Interleukin-6 biology is coordinated by membrane-bound and soluble receptors: role in inflammation and cancer. J Leukoc Biol 2006; 80: 227-236.
[29] Hirano T, Ishihara K and Hibi M. Roles of STAT3 in mediating the cell growth, differentiation and survival signals relayed through the IL-6 family of cytokine receptors. Oncogene 2000; 19: 2548-2556.
[30] Chang B, Smith RS, Hawes NL, Anderson MG, Zabaleta A, Savinova O, Roderick TH, Heckenlively JR, Davisson MT and John SW. Interacting loci cause severe iris atrophy and glaucoma in DBA/2J mice. Nat Genet 1999; 21: 405-409.
[31] Anderson MG, Smith RS, Hawes NL, Zabaleta A, Chang B, Wiggs JL and John SW. Mutations in genes encoding melanosomal proteins cause pigmentary glaucoma in DBA/2J mice. Nat Genet 2002; 30: 81-85.
[32] John SW, Smith RS, Savinova OV, Hawes NL, Chang B, Turnbull D, Davisson M, Roderick TH and Heckenlively JR. Essential iris atrophy, pigment dispersion, and glaucoma in DBA/2J mice. Invest Ophthalmol Vis Sci 1998; 39: 951-962.
[33] Inman DM, Sappington RM, Horner PJ and Calkins DJ. Quantitative correlation of optic nerve pathology with ocular pressure and corneal thickness in the DBA/2 mouse model of glaucoma. Invest Ophthalmol Vis Sci 2006; 47: 986-996.
[34] Weinreb RN and Khaw PT. Primary open-angle glaucoma. Lancet 2004; 363: 1711-1720.
[35] Crish SD, Sappington RM, Inman DM, Horner PJ and Calkins DJ. Distal axonopathy with structural persistence in glaucomatous neurodegeneration. Proc Natl Acad Sci U S A 2010; 107: 5196-5201.
[36] Sappington RM, Sidorova T, Long DJ and Calkins DJ. TRPV1: contribution to retinal ganglion cell apoptosis and increased intracellular Ca2+ with exposure to hydrostatic pressure. Invest Ophthalmol Vis Sci 2009; 50: 717-728.
[37] Choi JH and Won MH. Microglia in the normally aged hippocampus. Lab Anim Res 2011; 27: 181-187.
[38] Harry GJ and Kraft AD. Microglia in the developing brain: a potential target with lifetime effects. Neurotoxicology 2012; 33: 191-206.
[39] Gemma C, Bachstetter AD and Bickford PC. Neuron-Microglia Dialogue and Hippocampal Neurogenesis in the Aged Brain. Aging Dis 2010; 1: 232-244.
[40] Czeh M, Gressens P and Kaindl AM. The yin and yang of microglia. Dev Neurosci 2011; 33: 199-209.
[41] Soto I, Pease ME, Son JL, Shi X, Quigley HA and Marsh-Armstrong N. Retinal ganglion cell loss in a rat ocular hypertension model is sectorial and involves early optic nerve axon loss. Invest Ophthalmol Vis Sci 2011; 52: 434-441.
[42] Shea TB and Chan WK. Regulation of neurofilament dynamics by phosphorylation. Eur J Neurosci 2008; 27: 1893-1901.
[43] Schlamp CL, Li Y, Dietz JA, Janssen KT and Nickells RW. Progressive ganglion cell loss and optic nerve degeneration in DBA/2J mice is variable and asymmetric. BMC Neurosci 2006; 7: 66.
[44] Filippopoulos T, Danias J, Chen B, Podos SM and Mittag TW. Topographic and morphologic analyses of retinal ganglion cell loss in old DBA/2NNia mice. Invest Ophthalmol Vis Sci 2006; 47: 1968-1974.
[45] Jakobs TC, Libby RT, Ben Y, John SW and Masland RH. Retinal ganglion cell degeneration is topological but not cell type specific in DBA/2J mice. J Cell Biol 2005; 171: 313-325.